CRS stack based seismic imaging – a case study from St Ives mining camp, Kambalda, Western Australia

L.Malovichko
Department of Exploration Geophysics
Curtin University of Technology
26 Dick Perry Ave
Kensington, WA, 6015
liliya.malovichko@curtin.edu.au

M.Urosevic
Department of Exploration Geophysics
Curtin University of Technology
26 Dick Perry Ave
Kensington, WA, 6015
M.Urosevic@curtin.edu.au

SUMMARY

The Common Reflection Surface (CRS) stacking has been established as an alternative to conventional data-driven imaging techniques. We have successfully applied the CRS stacking technique to real 2D and 3D seismic data. A case study performed in the St Ives mining camp, Kambalda, Western Australia (WA) demonstrates that CRS stacking significantly improves imaging results and increases the effectiveness of interpretation steps. The CRS approach is now routinely used in hard rock seismic processing.

The main objective of this study is to review the application of the CRS approach at the St Ives mining camp in Kambalda, WA.

Key words: hard rock seismic exploration, CRS stack, seismic data processing.

INTRODUCTION

Seismic exploration in hard rock environments is challenging due to complex geological conditions that reduce the signal-to-noise (S/N) ratio of seismic data and, thus, an accurate velocity model recovery likelihood. This limits the application of conventional imaging methods, e.g., normal moveout (NMO), dip moveout (DMO) stacking or pre-stack migration.

The common reflection surface (CRS) stacking technique can be used in complex environments to increase the fold and therefore the signal quality and produces reliable stacked sections with high resolution (Gierse et al. 2003; Heilmann et al. 2004). The CRS stacking approach does not depend on a velocity model.

A number of pre-processing steps must be applied to seismic reflection data to construct an accurate CRS stack. These include: geometry setup, muting of bad shot and receiver gathers, f filtering, f-k filtering, deconvolution, field static correction, and amplitude correction.

The CRS stacking approach was applied to 2D and 3D datasets acquired across the St Ives mining camp in Kambalda, Western Australia located within the core of a regional-scale Kambalda Dome. Kambalda is one of the most prolific nickel and gold provinces in Western Australia. The deposits of this type are usually found in complex geological structures hidden by a deep, heterogeneous, and often conductive regolith stratum. This limits the depth of penetration for potential field methods, but at the same time allows new possibilities for the application of seismic methods.

METHOD AND RESULTS

The CRS stacking operator is based on three wavefront attributes in contrast to the CMP stacking operator (using just one - NMO velocities), and involves many more traces than those present in a CMP gather (Fig. 1). Conventional stacking velocity analysis and CMP stacking are limited by the CMP gather, where the travel time curve for a reflected wave is given by the equation

$$(1)\quad t^2 = t_0^2 + \frac{x^2}{V_{NMO}^2}.$$

In equation (1) t_0 is the zero-offset travel time at a particular source-receiver offset x. The parameter V_{NMO} is known as the NMO velocity.

In the CRS approach, assuming reflector continuity, we are stacking any reflection event that originates from a common reflection surface. The travel time curve in the midpoint-offset domain depends on three parameters instead of the single-parameter curve within a single CMP gather and is given by

$$(2)\quad t^2(\Delta m, h) = \underbrace{t_0^2 + \frac{x^2}{V_{NMO}^2}}_{equation\ (1)} + \underbrace{\frac{\Delta m^2}{V_{CMO}^2}}_{curv.dep.} + \underbrace{4t_0 p\Delta m + 4p^2\Delta m^2}_{dip\ dependent},$$

where x is the source-receiver offset, Δm is the relative midpoint coordinate, p is the horizontal slowness, and V_{CMO} describes a curvature-moveout velocity.
In two dimensions one can reformulate equation (2) as:

$$(3)\quad t_{CRS}^2 = \left(t_0 + \frac{2\cdot\sin\beta}{v_0}\Delta m\right)^2 + \frac{2t_0\cos^2\beta}{v_0}\left(\frac{h^2}{R_{NIP}} + \frac{\Delta m^2}{R_N}\right),$$

where v_0 is the near surface velocity, β is the angle-of-emergence or dip of a zero-offset wavefront, R_N is the instantaneous radius of the zero-offset wavefront and R_{NIP} is the instantaneous radius of curvature of the wavefront in the offset dimension.

2D dataset example

An experimental 2D seismic reflection dataset was acquired in 2005 over the McLeay nickel deposits, Lake Lefroy, Kambalda, WA (Urosevic *et al*. 2005). The main objective was to map deep complex structures associated with the Kambalda Dome. Eleven 2D seismic lines of total length 82.4 km were acquired. The receiver increment was 10 m, shot increment was 20 m. The pre-processing steps were: trace editing, static correction, amplitude recovery, f-k filtering, spiking deconvolution, velocity analysis, residual statics, velocity analysis and muting. Due to the high noise level of this dataset difficulties were encountered during conventional processing using the CMP (NMO/DMO) stack or prestack time migration methods. As an example of a conventional stack in Fig. 1 (right bottom), we show the poststack depth-migrated CMP stack with NMO/DMO corrections. It is of low quality, with few seismic reflections in the central part.

To apply the CRS stacking approach, we used the same pre-processed data as for the CMP (NMO/DMO) stacking. The Z0 section simulated by means of the CRS stack along with the coherence section and dips β (3) attribute sections are shown in Fig. 2.

The comparison between poststack depth-migrated results of conventional NMO/DMO stack (left) and CRS Z0 stack (right) is shown in Fig. 3. One can see a noticeable improvement in the CRS stacked section compared to the conventional CMP (NMO/DMO) stacked section. The CRS stacked result shows better S/N ratio and continuity of seismic events, mainly in the upper part of the section and in strongly dipping reflections.

3D dataset example

The 3D seismic survey was conducted in 2007. Data was acquired above the Beta Hunt nickel mine on Lake Lefroy, south of the Kambalda township. The 3D survey area was located between abandoned gold mine pits, mullock heaps, dikes and mine infrastructure. The total area covered by the shot and receiver lines was approximately 3.5 km^2. The distance between source and receiver lines was ~90 m. Small explosive charges (110 g) were deployed in 1.2-1.5 m deep holes. The data was processed to stacked and migrated volumes using the workflow described by Urosevic et al (2012). The volumes consist of 165 inlines and 190 xlines, bin size is 10x10 m, average fold in the central part is over 80.

In three dimensions, up to eight different parameters are used to describe the CRS. Searching for these parameters would be time consuming. Thus, only three parameters are used: dip β, azimuth α, and R_{NIP}, which is represented as an RMS velocity. Four inlines from the depth-migrated CRS stacked 3D volume are shown in Fig. 4 (bottom). Fig. 4 (top) contains inlines from the conventional post-stacked depth-migrated 3D volume. Inlines from depth-migrated CRS stacked 3D volume show significant improvement in the S/N ratio and lateral continuity of seismic events.

CONCLUSIONS

In this work CRS processing has provided a significant improvement in the S/N ratio. This was demonstrated using three 2D seismic sections and a 3D seismic volume. Stacked 2D seismic sections and a 3D seismic volume obtained using the CRS approach are superior to those obtained by conventional DMO/NMO processing. They are characterized by a higher S/N ratio and improved continuity of seismic reflection events. Parameters (wavefield attributes) estimated using the CRS approach have a clear geophysical interpretation and will be used for building velocity models.

The target area and the existing faults and fractures were imaged clearly and the high grade of tectonic displacement necessary to ensure a sufficiently large production rate was verified. The CRS approach is now adopted as a part of the standard processing flow for hard rock seismic.

ACKNOWLEDGMENTS

This research was carried out at Curtin University in the Department of Exploration Geophysics. The work was supported by the Deep Exploration Technologies Cooperative Research Centre whose activities are funded by the Australian Government's Cooperative Research Centre Programme. The authors thank their colleagues, and in particular Roman Pevzner, Andrej Bona and Anton Kepic for their contribution to this study.

REFERENCES

Gierse, G., Pruessmann, J., Eisenberg-Klein, G., Caballero, A., Ballesteros, R. and Clemente, G., 2009, Improved Salt Delineation by CRS-based Depth Model Building and Depth Migration: 71st Annual International Conference and Exhibition, EAGE, Expanded Abstracts, Session Z-85.

Heilmann, Z., Mann, J. and Koglin, I., 2006, CRS-stack-based seismic imaging considering top-surface topography: Geophysical Prospecting, 54, 681-695.

Jager, R., Mann, J., Hocht, G. and Hubral, P., 2001, Common-Reflection-Surface stack: image and attributes: Geophysics, 66(1), 97-109.

Mann, J., Jager, R., Muller, T., Hocht, G. and Hubral, P., 1999, Common-reflection-surface stack – a real data example: Journal

Mann, J., Schleicher, J. and Hertweck, T., 2007, CRS Stacking – A Simplified Explanation: 69th Annual International Conference and Exhibition, EAGE, Expanded Abstracts, Session B044.

Urosevic, M., Bhat, G. and Grochau, M., 2012, Targeting nickel sulfide deposits from 3D seismic reflection data at Kambalda, Australia: Geophysics, 77, 123-132.

Urosevic. M., Stolz. E. and Massey. S., 2005, Seismic exploration of complex mineral deposits - Yilgarn Craton, Western Australia: *67th EAGE Annual International Conference and Exhibition*, Expanded Abstracts, Session Z-99.

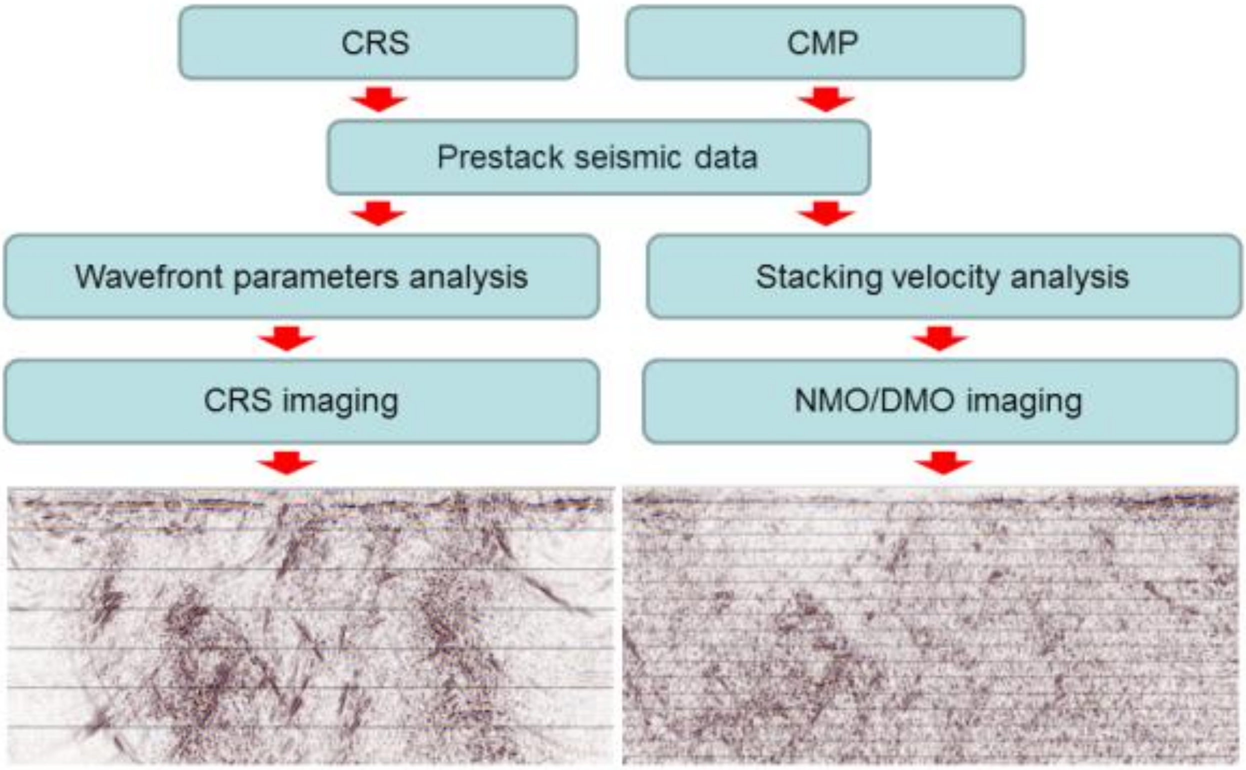

Figure 1. Schematic representation of conventional and CRS stack imaging, highlighting the main difference between stacking operators. Conventional stacking is performed in individual CMP gathers and is based on stacking velocity V_{NMO} analysis. CRS stacking involves many more traces than those present in a CMP gather and based on three wavefront parameters analysis: the angle-of-emergence or dip of a zero-offset wavefront β, the instantaneous radius of the zero-offset wavefront R_N and the instantaneous radius of curvature of the wavefront in the offset dimension R_{NIP}. Seismic sections in the depth domain are showing an example of a 2D seismic line (SI_NJ1, Kambalda Nickel field)

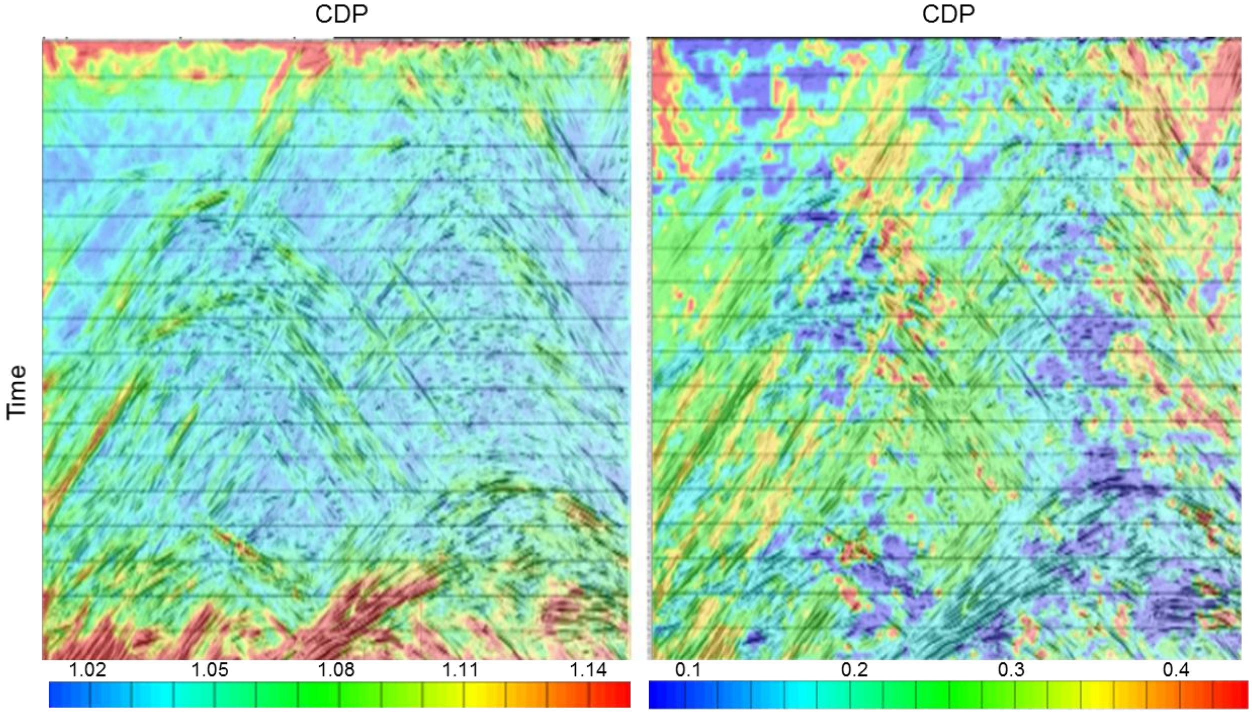

Figure 2. 2D line (SI_CR1, Kambalda Nickel field) example. Coherency section (left), showing a measure of fitting of CRS operator to the data, and an emergence angle or dips (right) of the Z0 ray at the surface. Blue colour (left) denotes regions with low coherence.

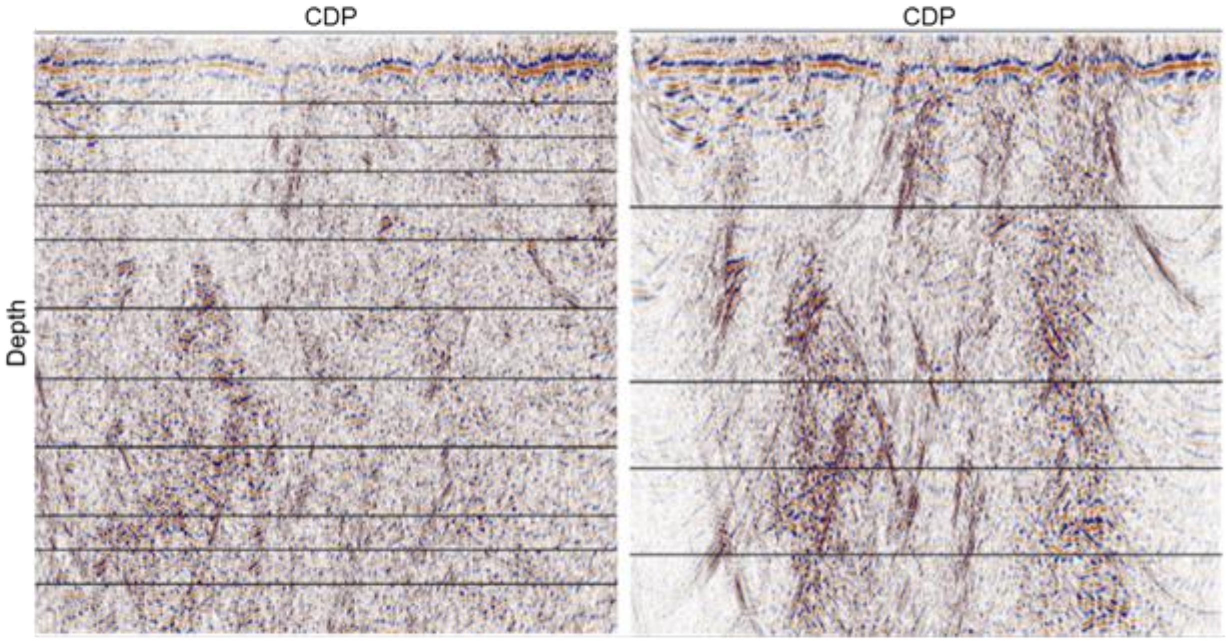

Figure 3. 2D line (SI_CR1, Kambalda Nickel field) example. Comparison between poststack depth-migrated results of conventional NMO/DMO stack (left) and CRS Z0 stack (right)

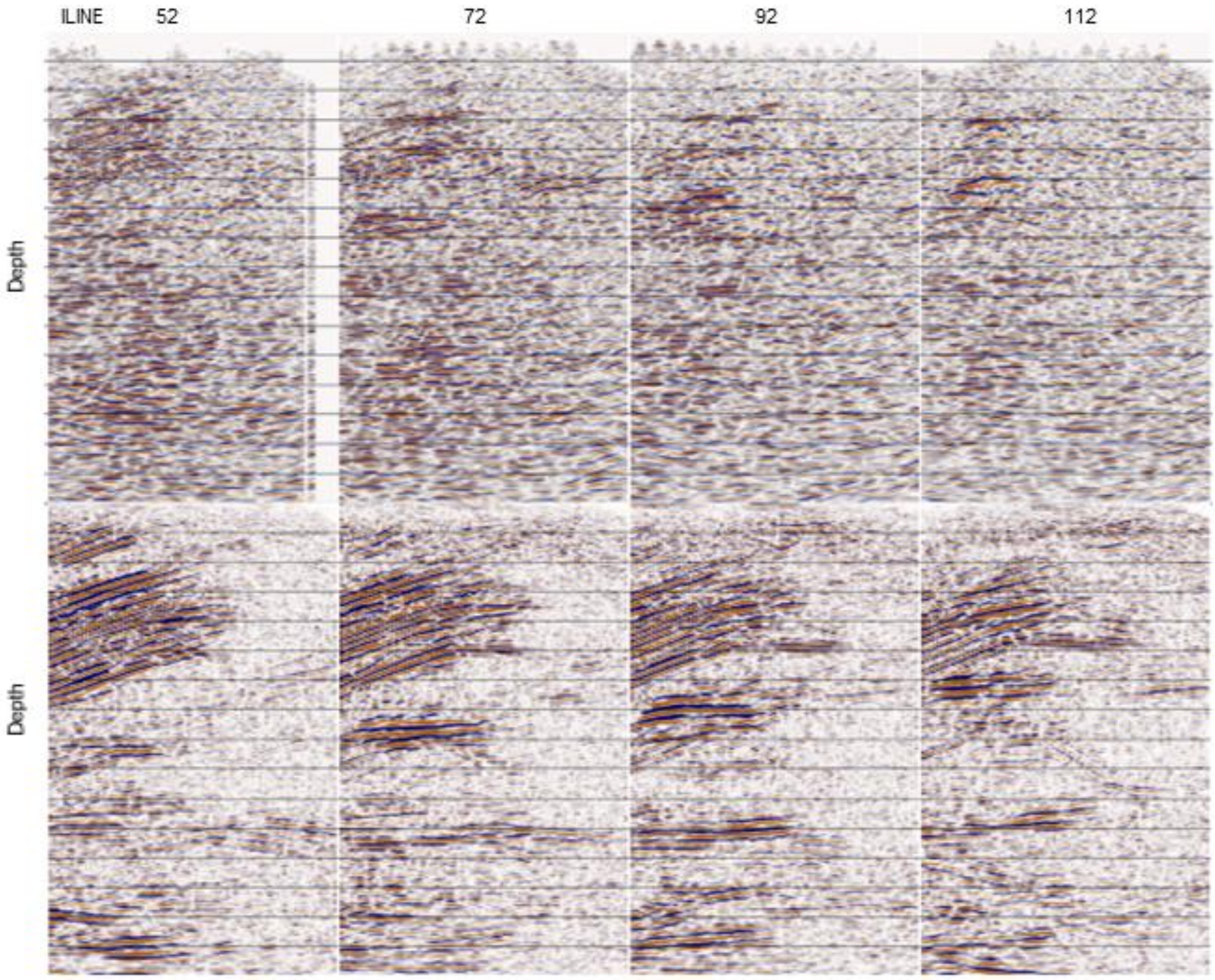

Figure 4. 3D survey example (CM3D_07). Inlines 52, 72, 92, 112 from conventional (top) and CRS (bottom) post-stacked depth-migrated volumes